# MECHANISTIC MODELING OF TWO-PHASE FLOW AROUND SPACER GRIDS WITH MIXING VANES

**B. M. Waite, D. R. Shaver and M. Z. Podowski**
Department of Mechanical, Aerospace and Nuclear Engineering, Rensselaer Polytechnic Institute,
110 8th Street, Troy, NY 12180, USA
waiteb2@rpi.edu, shaved2@rpi.edu, podowm@rpi.edu

## ABSTRACT

Spacer grids in nuclear reactor fuel assemblies may have a significant effect on coolant flow and heat transfer within the reactor core. There has been a great deal of work carried out by the nuclear power industry to optimize spacer designs to improve reactor performance during both normal and accident conditions. Many of these designs employ mixing devices in order to enhance the heat transfer within the core. The effect of fuel rod spacer grids can be even more significant at multiphase flow conditions. The challenges associated with the modeling of two-phase flow and heat transfer with phase change in the spacer region are augmented by the complexity of the geometry that gives rise to both numerical and theoretical issues.

The overall objective of the present study has been to develop a consistent multidimensional model and the corresponding solution methodology for the analysis of two-phase flows around mixing vanes in reactor subchannels. The proposed model has been implemented in a state-of-the-art computational multiphase fluid dynamics code, NPHASE-CMFD. This code uses a pressure-based finite volume solution method which is applied to RANS-level ensemble-average multifield equations of multiphase/multi-component fluids. It has already been extensively applied and tested before to simulate both adiabatic and diabatic gas/liquid flows in complex geometries [1], [2], [3].

This main focus the work reported in this paper has been on the PWR spacer design with Split-Vane type mixing devices [4]. The results of NPHASE-CMFD-predicted evolution of the velocity field and void distribution between the upstream and downstream sections around the spacer are presented. The results of parametric testing on the effect of inlet conditions and of the vapor-generation rate along the heated fuel rods are also shown, as well as those of model verification and validation against experimental data.

**KEYWORDS**: Reactor spacer grids, mixing vanes, mechanistic two-fluid model of gas/liquid flows, local void fraction prediction

## 1. INTRODUCTION

The introduction of mixing devices into a pressurized water nuclear reactor core has allowed operators to increase reactor thermal limits and enhance system performance. While pressurized water reactors are designed to operate primarily at single phase flow conditions, localized boiling is actually still allowed in the hottest regions of the core. Understanding the effects of the mixing devices on boiling is key to correctly predicting temperatures and void distribution within the reactor core. Since void distribution has a significant effect on the heat transfer characteristics in reactor subchannels, special care should be taken in order to ensure accurate predictions. If such predictions can be successfully made for the region downstream of the spacer and mixing vanes, the results could be used in the future to design better mixing devices specifically for boiling heat transfer enhancement.

Significant efforts were made in the past to understand the effect of spacers, but a majority of work has been performed with only single phase heat transfer in mind. The investigations included spacer grids and mixing vanes designed to induce swirling flow, increase mixing between channels, or a combination of both phenomena [5], [6], [7]. Anglart et al. [8] published some of the first studies concerning the modeling of flow and phase distribution around spacers, but their work was mainly concerned with a BWR type design that employed no mixing device. There have been continuing interests, especially with increased computer capacity and more advanced experimental technology, to better understand how the mixing devices affect boiling flows. Wheeler et al. have reported experimental results showing how the presence of a spacer can actually shift the flow-regime due to coalescence and breakup [9]. The NUPEC PWR Subchannel and Bundle Study included a multitude of tests on full scale mock-ups to provide void fraction data in order to check the accuracy of numerical simulations [10]. CD-Adapco have performed numerical simulations using the STAR-CCM+ code [11], which were focused on the average void prediction in the spacer region. Areva also used STAR-CCM+ to examine the source terms for the interfacial area transport equation. [12].

Most recently, Ylönen presented adiabatic air-water flow data from the SUBFLOW facility at ETH-Zurich [13], which used a wire mesh sensor to measure lateral void fraction distributions downstream from a spacer, based upon the geometry of Navarro et al., [4]. This data is rare in the literature and useful for benchmarking CFD models. While the method is intrusive to the flow and has limitations to the size of bubbles it can measure, it provides consistent insight into where the void is expected to be both along and downstream of the mixing vanes. Unfortunately, the farthest measurements were taken only about 21 hydraulic diameters downstream of the spacer, whereas the developing length of two-phase flows can be much longer. In collaboration between Areva and ETH-Zurich, Goodheart et al. [14] again used the commercial CFD code, STAR-CCM+, to perform CFD simulations for the conditions corresponding to those in the ETH experiments.

The current work is part of continuing efforts at RPI to develop, test and validate a complete mechanistic multifield model of gas (vapor)/liquid flow and heat transfer [15], and to demonstrate its applicability to capture the physical mechanisms governing phase distribution in the subchannels of light water nuclear reactors (LWR). Specifically, the focus of the investigations documented in this paper has been on evaluating general models of two-phase flow, which have originally been developed for smooth conduits, for application to flows around mixing vanes in PWRs. Capitalizing on the results of the earlier preliminary works which demonstrated the applicability of such models to flows around local obstructions [16] and simplified spacer grids [17], the current study concentrates on two-phase flows around spacers with a split-vane-type mixing geometry. The predictions of the current model have been compared against the experimental results of Ylönen [13].

## 2. MODEL FORMULATION

As mentioned in the Introduction section, the current modeling approach is based on a theoretical formulation of multifluid ensemble-averaged equations governing the fluid mechanics and heat transfer of gas (vapor)/liquid two-phase flows. The emphasis is on using first-principle physical laws and on minimizing the number of adjustable coefficients which are commonly used in existing CFD models. To illustrate the modeling principles, the dispersed-flow momentum equation is discussed in Section 2.1.

The overall multifluid/multicomponent model has been implemented in the state-of-the-art computer code, NPHASE-CMFD. NPHASE-CMFD is a RANS-based, parallel processing Computational Multiphase Fluid Dynamics (CMFD)) solver. It uses a multifield modeling concept to solve the conservation of mass, momentum and energy equations, combined with the corresponding interfacial jump conditions, for each individual fluid component. Both segregated and coupled numerical solution methods are available for this purpose [18]. The model also includes the transport equations for turbulence quantities and chemical species. These modeling capabilities of the NPHASE-CMFD solver have been extensively validated before against experimental data.

## 2.1. Equations Governing Two-Phase Flow

A consistent two-fluid model of dispersed, adiabatic gas/liquid flows has been used to simulate the posed problem in NPHASE-CMFD. A general form of the phasic momentum conservation equations for this model is given by

$$\frac{\partial}{\partial t}\left(\alpha_j \rho_j\right) + \nabla \cdot \left(\alpha_j \rho_j \vec{u}_j\right) = 0 \tag{1}$$

$$\frac{\partial}{\partial t}\left(\alpha_j \rho_j \vec{u}_j\right) + \nabla \cdot \left(\alpha_j \rho_j \vec{u}_j \vec{u}_j\right) = -\alpha_j \nabla P + \alpha_j \nabla \cdot \left[\underline{\underline{\tau}}_{lam} + \underline{\underline{\tau}}_{turb}\right] + \vec{F}_{k-j} \tag{2}$$

where the subscripts j and *k* are the field indicators (i.e. *l* and *v*).

It should be noted that both fluid fields are affected by the continuous (liquid) field shear and pressure. The models for the interfacial forces, $\vec{F}_{l-v}$, used in this study are implemented based on the formulation applicable to bubbly flows with relatively small bubble diameters. The drag force can be expressed as

$$\vec{F}_{d,l-v} = -\frac{3}{4}\frac{C_d}{D_b}\alpha_v \rho_l \left|\vec{u}_v - \vec{u}_l\right|\left(\vec{u}_v - \vec{u}_l\right) \tag{3}$$

where the drag coefficient is determined as a function of the relative Reynolds number for a bubble using the expression proposed by Podowski [19] (which is a modified form of that by Ishii and Chawla [20])

$$C_d = \frac{24}{\mathrm{Re}_b}\left(1 + 0.092\,\mathrm{Re}_b^{0.78}\right) \tag{4}$$

The virtual mass force is given by the following expression [1].

$$\vec{F}_{vm,l-v} = -C_{vm}\alpha_v \rho_l \left(\frac{D\vec{u}_v}{Dt} - \frac{D\vec{u}_l}{Dt}\right) \tag{5}$$

where $C_{vm}$=0.5 is used. This force resists bubble acceleration which aids in the stabilization of flow around the mixing vanes.

The formulation for the lift force acting on the bubbles is

$$\vec{F}_{L,l-v} = -C_L \alpha_v \rho_l \left(\vec{u}_v - \vec{u}_l\right) \times \left(\nabla \times \vec{u}_l\right) \tag{6}$$

where the lift coefficient is constant at 0.09 more than one bubble diameter away from the wall and then decreases linearly to zero toward the wall. This formulation is consistent with the modeling work done by Jiao and Podowski [22] and the value has been determined from parametric testing against experimental data [23]. The turbulent dispersion force on the bubbles is used as proposed by Podowski [24].

$$\vec{F}_{TD,l-v} = -C_{TD}\alpha_v \rho_l \kappa_l \nabla \alpha_v \tag{7}$$

where the coefficient of turbulent dispersion has been mechanistically determined to be 2/3 and $\kappa_l$ represents the turbulent kinetic energy of the liquid component.

The above formulation of two-phase flow has been shown to be consistent through parametric testing against experimental data [25]. The present model relies on *a priori* determination of the bubble diameter as well as the lift and turbulent dispersion coefficients. These assumptions may have a significant effect on the developing flow after the mixing vane.

## 2.1. Geometry

While the actual geometry of coolant channels in a nuclear reactor core is complex with springs, dimples and extra flow paths within the spacers, the main objective of the current model is to capture the major characteristics of PWR spacer geometry; in particular, the effect of split-vane-shaped skewed geometry on secondary flow and phase redistributions. The basic spacer dimensions have been specified based on the information provided by Navarro et al. [4]. A representation of the mixing-vane and spacer combination is shown in Figure 1. The hydraulic diameter, $D_H$, for this geometry is 1.202 cm (12.7 mm pitch and 9.53 mm rod diameter), and the 1 cm long fins are bent 25 degrees away from the axial flow direction, causing a flow obstruction. In the simulations, the outlet section after the spacer has been 50 cm long in order to allow for flow redevelopment.

**Figure 1. Spacer with split-vane mixing device.**

### 2.1.1. Grid formulation

Multiple grids have been used with the same topology (i.e. distribution of elements) in the lateral plane to reduce computational costs. In this way, the fully-developed flow conditions can be reached in a bare-channel without a spacer, and then used as an inlet condition for a domain with the spacer. Keeping the topology consistent for the inlet and outlet sections of the grid with the spacer allows the flow to be recycled back into the inlet of the spacer domain or into the bare-channel domain in order to study the void distribution downstream of the spacer. The mixing vane region has been formed with unstructured tetrahedral in order to accommodate the complexity of the geometry. The grid has been formulated with structured boundary layers of hexahedral elements on the fuel rod, spacer, and fin surfaces. Figure 2 shows two views of the computational domain used in this study.

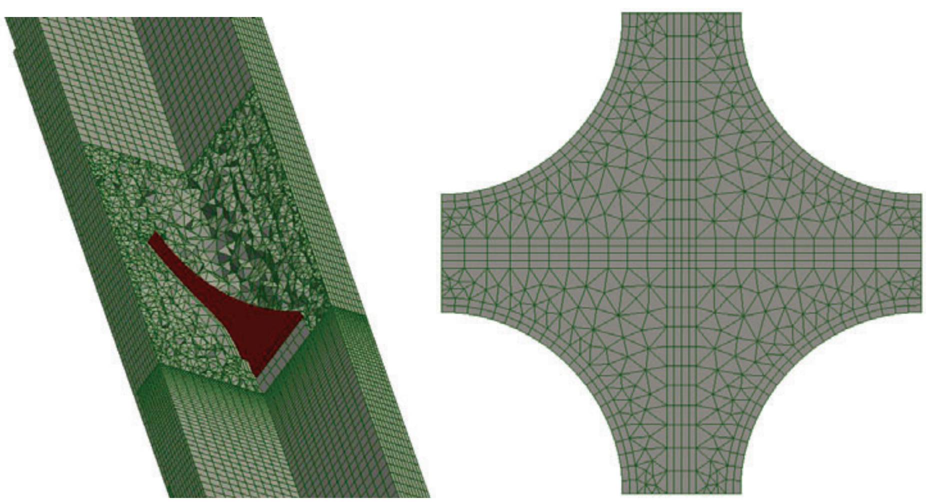

**Figure 2. Cross Sections of Grid Topology, Left: Cut of mixing vane region, Right: Lateral view of grid outside of mixing vanes.**

The narrow boundaries between the rods are modeled as symmetry planes. Another characteristic feature of the current computational domain is that the spacer and fin surfaces are modeled as thin no-slip walls. Neglecting the thickness eased the construction of the computational mesh as it also resulted in a slightly larger flow area in the narrow regions. This, in turn, allows for the investigation of effect of the fins themselves by separating it from that of the changing flow area. The domain for the single channel cases consisted of 783,112 cells which modeled the 60 cm long geometry. The runs completed 2000 iterations in approximately 15-16 hours with 8 CPUs. The computational methodology employed allows for larger domains to be studied with a moderate computational cost.

## 3. RESULTS

### 3.1. Vapor Injected at the Inlet

The objective of the simulations has been to determine the effect of the fins on the flow and void distributions inside and around the spacers. The initial study has focused on low-void-fraction flows with relatively small bubbles, to get an understanding on how the computational model responds to the presence of the mixing vanes. This focus has also allowed for a parametric study on how selected modeling factors, such as the value of the lift coefficient, might affect the flow. Table 1 shows a summary of the conditions examined in this study. For all cases, the two phases are at thermal equilibrium. The steam/water cases are simulated at the saturation temperature corresponding to the prescribed pressure. With each respective case, only one variable was changed in order to compare the effects of the specific parameter. The “Base” case corresponds to 0.101 MPa, with a lift coefficient of 0.09, and is described first in Table 1. The bubble diameter for all cases was selected based upon the expected bubble size for typical PWR operating conditions. The high pressure case has a liquid velocity of about 1.5 m/s which is about 50 % of the rated flow in a typical PWR core.

**Table 1. Summary of Steam/Water Conditions**

| Case | P [MPa] | $Re_L$ | $j_l$ [m/s] | $j_v$ [m/s] | $D_b$ [mm] | $\alpha_{in,avg}$ | $\rho_l$ [kg/m$^3$] | $\rho_v$ [kg/m$^3$] | $C_L$ |
|---|---|---|---|---|---|---|---|---|---|
| Base | 0.101 | 60,000 | 1.468 | 0.1673 | 0.25 | 0.10 | 958.4 | 0.5975 | 0.09 |
| High $C_L$ | 0.101 | 60,000 | 1.468 | 0.1673 | 0.25 | 0.10 | 958.4 | 0.5975 | 0.2 |
| High P | 15.6 | 153527 | 1.468 | 0.1673 | 0.25 | 0.099 | 592.4 | 103 | 0.09 |

It has been first necessary to establish what a fully developed flow looks like in a single subchannel, in order to have a baseline to compare the mixing vane results to. To generate fully developed flow profiles, a bare channel was simulated, i.e. one without a spacer grid or mixing vanes. The inlet conditions were specified as flat profiles for the phasic velocities and void fraction. The results are shown in Figure 3 for conditions corresponding to the “Base” case, as contour plots on a plane normal to the principal flow direction at 91.5$D_H$ downstream of the inlet. As this case is for small bubbles, the void fraction shows the expected wall-peaked behavior and the liquid velocity experiences a dramatic drop in the narrow near-wall regions. The lift force pushes the bubbles to the side, which causes a slightly higher void fraction in the narrow gap than in the center of the subchannel.

Fully developed results similar to those shown in Figure 3 have then been used as the inlet conditions for the channel with the mixing vane and spacer. Figure 4 shows the locations at which the results are presented for the domain including the spacer and mixing vanes. There is a 5 cm inlet section followed by the spacer and then a 50 cm outlet section. The figure shows the fins as red, and the spacer grid that isolates the flow into 4 quarters colored in blue.

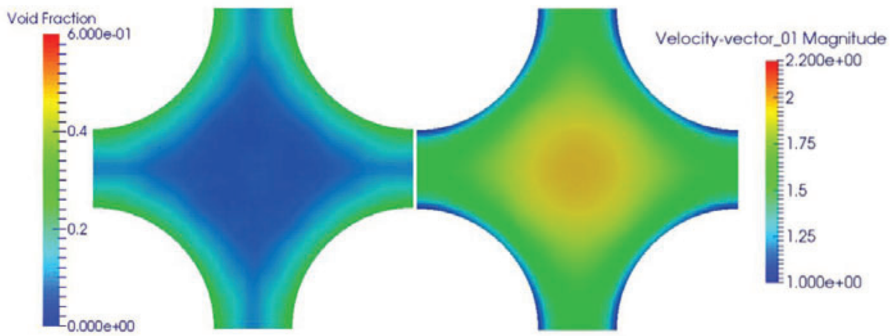


**Figure 3. Fully developed profiles for the base case (left) void and (right) liquid velocity.**

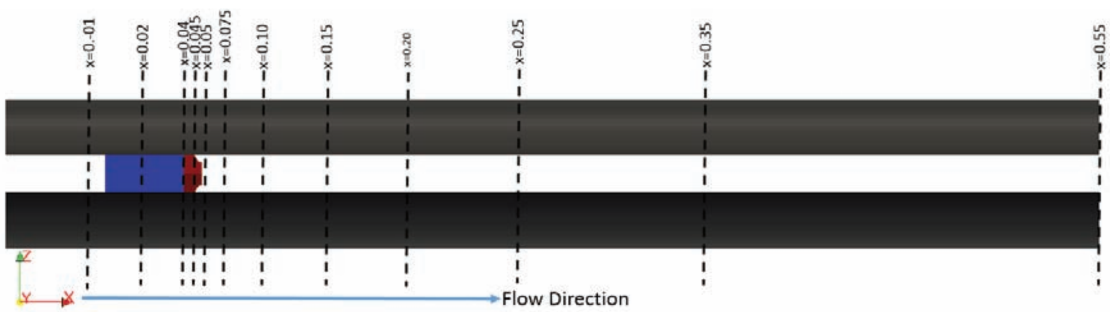


**Figure 4. Slice locations.**

The results are again presented as contour plots in a plane normal to the principal flow direction. These "slices" of the domain are taken closer together near the fins to show details of the effect of the fins on the flow. Figure 4 shows the results for the void fraction overlaid with the lateral velocity vectors, and the velocity magnitude at each slice.

Examining Figure 4, one can readily notice that the mixing vanes swirl the flow, which in turn causes the void to be carried away from the wall toward the center. Vortices are created by this effect, a large one in the center and a few smaller ones on the edges. The light steam is trapped in these vortices as the heavy liquid is swirling and being pushed outward by centripetal acceleration. This leaves the gas behind in the center of the vortices. Examining the progression downstream from the spacer, the smaller void concentrations are later overtaken by the larger swirl and brought toward the center. This causes a large peak in the center that remains even after the vortex has mostly decayed.

At x=0.25, the void is still concentrated in the center of the channel, but the velocity profile has practically returned to its fully developed form. This is evident from the void fraction and axial liquid velocity results shown in Figure 5, which presents line plots taken across the channel diagonal. It is clear that void fraction requires significantly more distance for the interfacial forces to return the void fraction to a fully developed profile. The void fraction peak slowly decreases downstream from the spacer while the axial liquid velocity reaches a practically fully-developed profile around 25 $D_H$ past the spacer. The void fraction has returned to a wall-peaked profile at about 87 $D_H$ downstream now that the lift and turbulent dispersion forces have had time to act on the vapor phase. While this behavior is what is expected from the current models, in reality the high peak in the center could have caused some coalescence resulting in larger bubbles that would remain in the center.

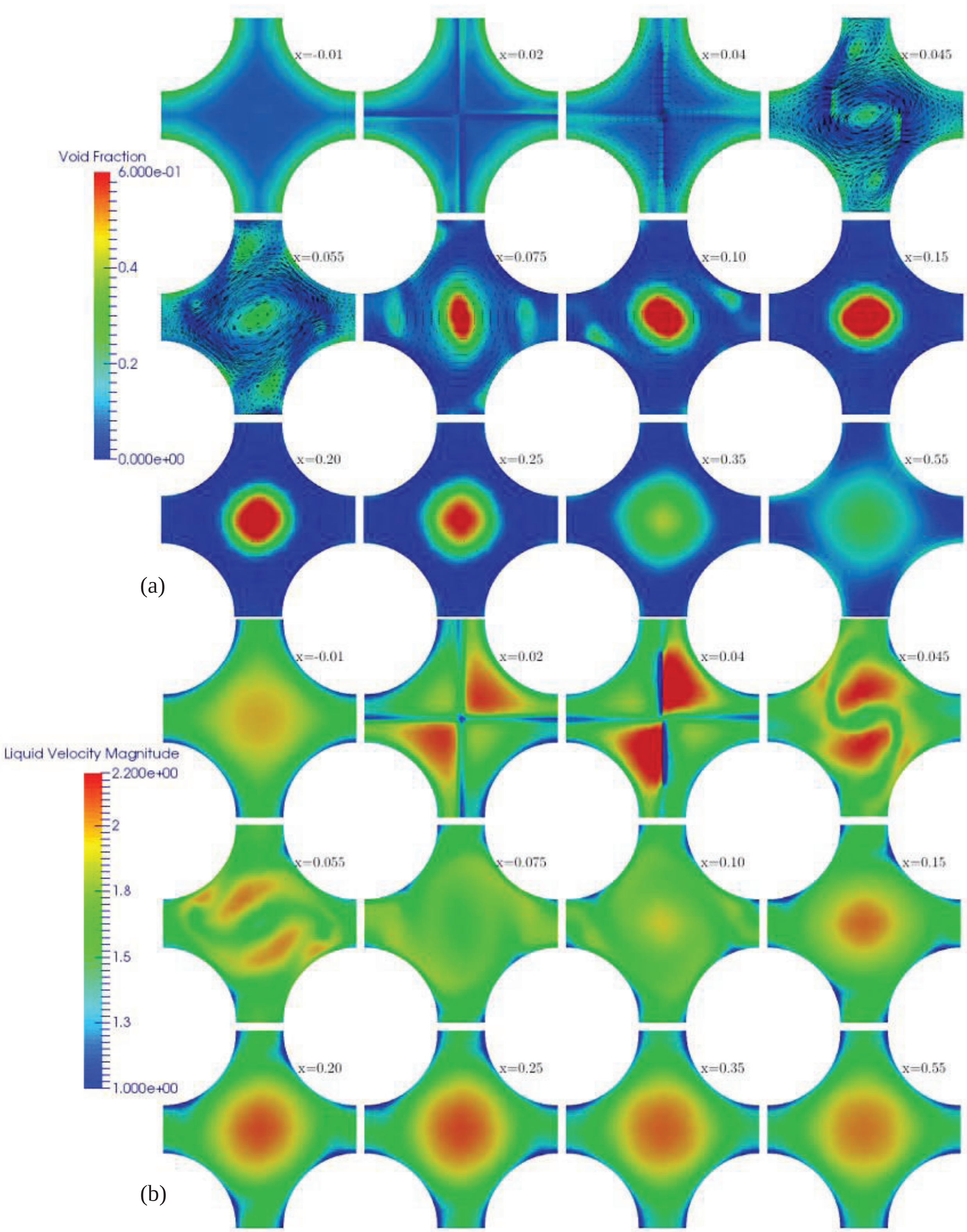


**Figure 5. Contour plots for the Base case, (a) void fraction with lateral velocity vector, (b) velocity magnitude.**

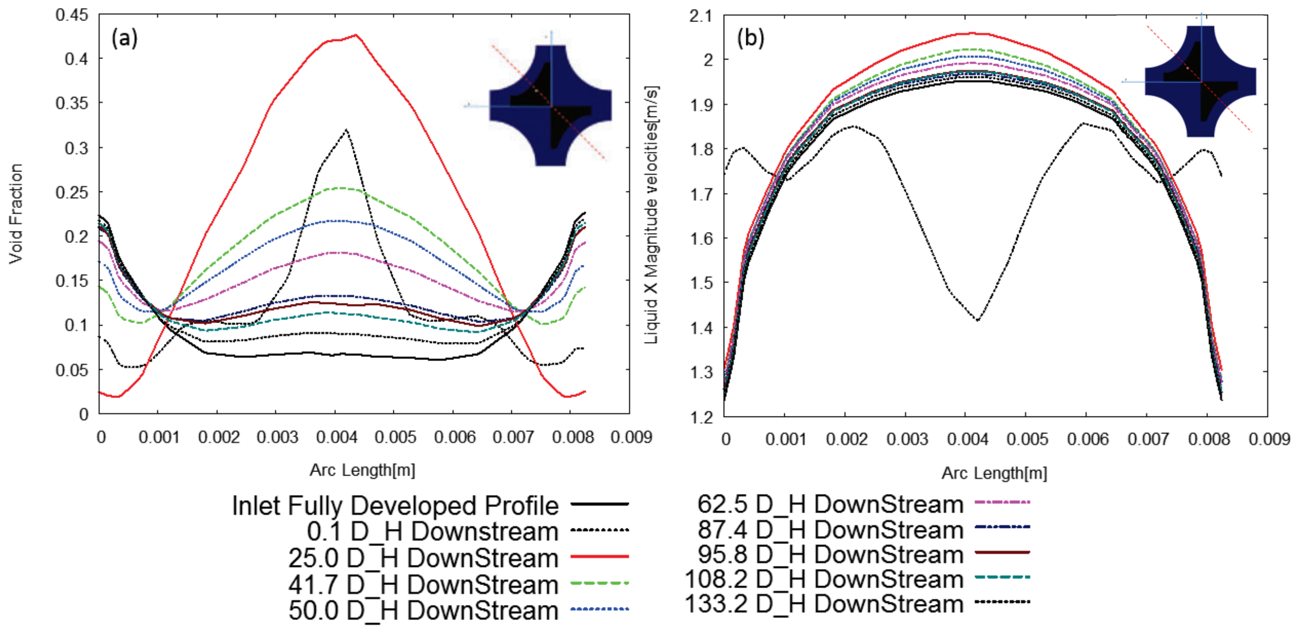


**Figure 6 . Redeveloping length with $C_L$=0.09 for the Base Case, (a) void fraction and (b) liquid axial velocity.**

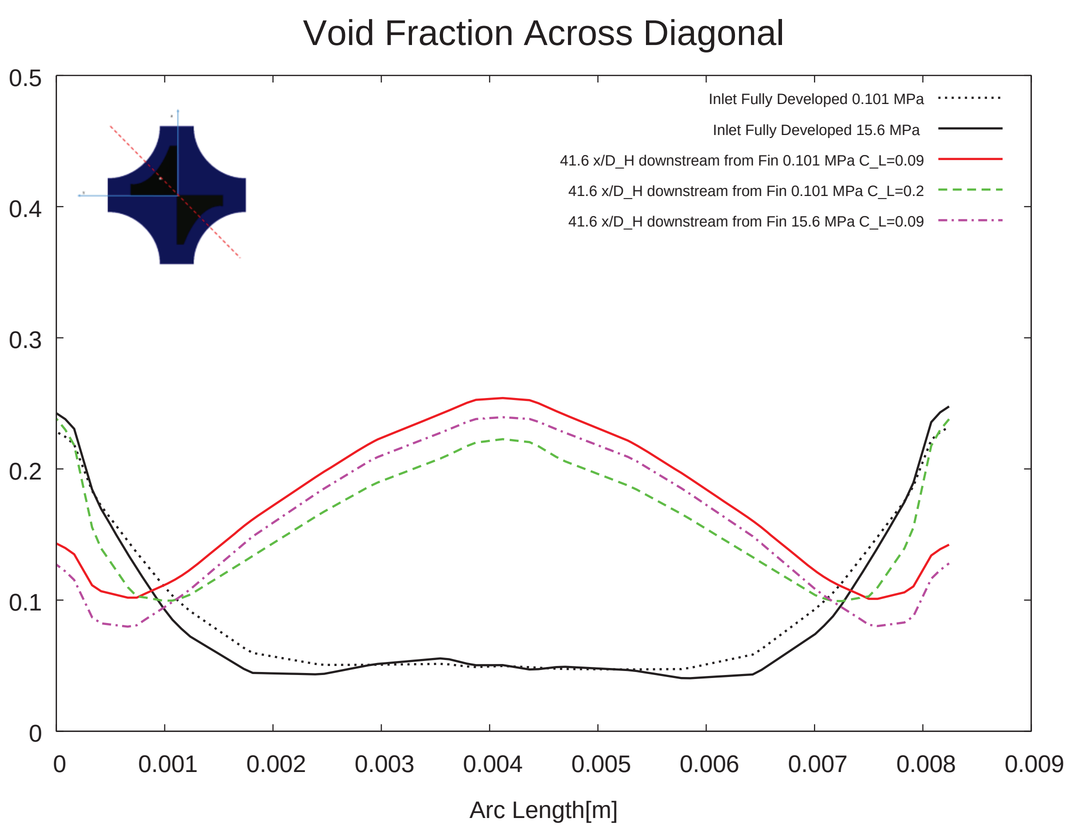


**Figure 7 . Results of the parametric study for the void fraction profile across the diagonal.**

Varying the parameters of the models allows one to improve the understanding of what forces are at play here. Additional cases have been run with a stronger lift coefficient, 0.2, as well as increasing the pressure to PWR reactor pressure, 15.6 MPa, in order to test the influence of the interfacial force models within the developing region. This brings the ratio of densities down from about 1000 to around 6. In close proximity to the mixing vanes, the effects of the interfacial forces are outweighed by the effects of the mixing vanes so the results in this region are practically independent of the model parameters.

The results from the parametric study are directly compared in Figure 6. This shows void fraction profiles for all three cases. From Figure 5a, it is concluded that the lower the peak of the void fraction is in the center, the closer to fully-developed the flow has become. From Figure 6, it can be seen that the case with the larger lift coefficient is closest to fully-developed conditions described in Figure 7. It is also shown that decreasing the density ratio has little effect on the shape of the void fraction profile and only shifts its magnitude. However, the effects of both changes are rather small, only reducing the peak by 2-3 %.

### 3.1.1. Comparison between experimental data and predictions

Any numerical study requires a comparison against real data or validated/accepted reference analyses to provide confidence in the results. A qualitative comparison has been performed with the wire mesh sensor results done at ETH-Zurich [13]. The experiments were carried out for air/water mixture at atmospheric pressure and a temperature of 23°C. The case simulated has a superficial liquid velocity of 0.8 m/s, a superficial vapor velocity of 0.039 m/s and uses a bubble diameter of 2 mm. The computational grid dimensions were scaled by a factor of 2.6 for a direct comparison to the Ylönen experiment. The experiment was scaled by the original investigator because 2.6 is the ratio between the critical bubble diameter at reactor steam/water conditions to atmospheric air/water conditions, as well as for ease of taking measurements. The results of simulations are shown in Figure 8.

The left hand side of Figure 8 has been reproduced from Ref. [13], and a single subchannel simulation done with NPHASE-CMFD is shown on the right hand side. Each row of results show a different axial cut plane, listing from top to bottom they are 50, 250 and 450 mm downstream from the spacer. The single-subchannel simulation is symmetrical and captures no effects of flow between subchannels. This allows the void to be coherently in the center of the channel until the interfacial forces redistribute the void. However effects of cross flow can clearly be seen in the experimental data as the void concentrations appear to be off center. The mixing vanes' orientation are alternated in the 4x4 channel experiment meaning that some of the channels fins are not in the same orientation as the one-channel geometry simulated which makes a direct qualitative comparison somewhat difficult. The single channel simulation agrees more with the outside channels where the effects of cross flow are smaller due to flow boundary walls. On average, the current model is slightly over-predicting the void concentration at all three downstream locations. This effect continues to grow as the flow progresses further downstream past 450 mm. One of the possible reasons is the actual distribution of bubble sizes.

It has been assumed in the simulations that the diameter of bubbles is 2 mm. While no detailed bubble size analysis has been performed on this case in the experiment, an analysis of a rod bundle without a spacer stated that the bubble distribution for similar flow rates had a distribution ranging from 2 mm to 9 mm [13]. This puts the assumption at the lower end of the spectrum of what bubble diameters could actually be present. The selection of the smaller bubble size is due to the applicability of the current models to small spherical bubbles only. The difference between the modeling assumption of 2 mm and the vast distribution in the experiment explains the differences in downstream distributions because the larger bubbles will be pushed toward the center by the interfacial forces unlike the smaller bubbles in the computer simulation. This also explains why the simulations predict a slightly higher concentration of bubbles in the center of the channel. Namely, smaller bubbles have a lower relative velocity and must have a higher void fraction for a given superficial velocity.

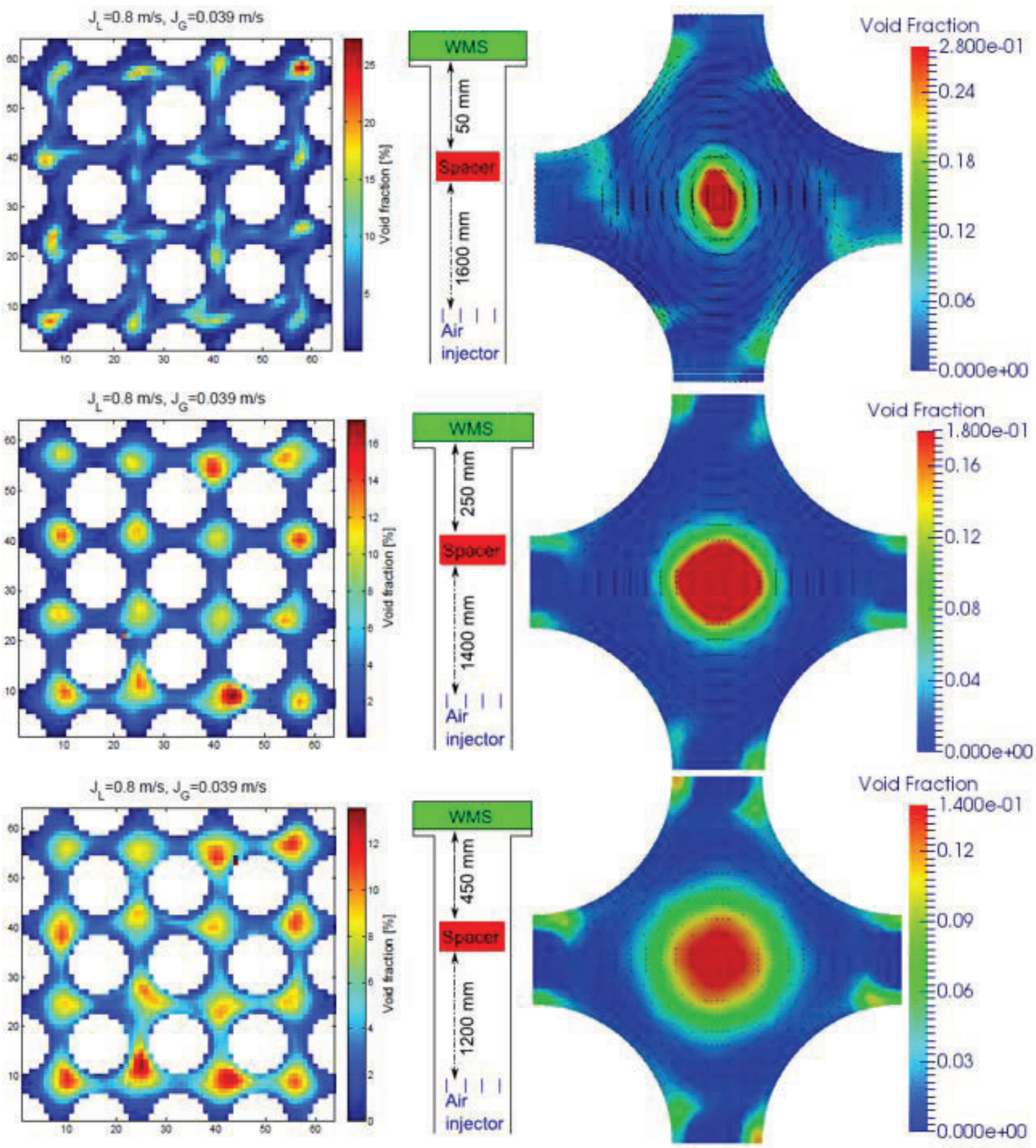


**Figure 8. Comparison of single channel results (Cut Planes; Top: 50mm, Middle: 250 mm, Bottom: 450 mm). Left: figures reproduced from Ylönen [13], Right: results from NPHASE-CMFD.**

To extend the comparison, four interconnected subchannels have been simulated as well, to account for cross flows between the inter-communicating channels. The boundary conditions in the outer rod gaps are symmetry conditions. The vanes have been rotated 90 degrees from each other so the symmetry plane is on the diagonal. This arrangement agrees with that for the four center channels in the experiment. The vane arrangement, and the predicted void distribution 50 mm downstream with lateral velocity vectors, are shown in Figure 9.

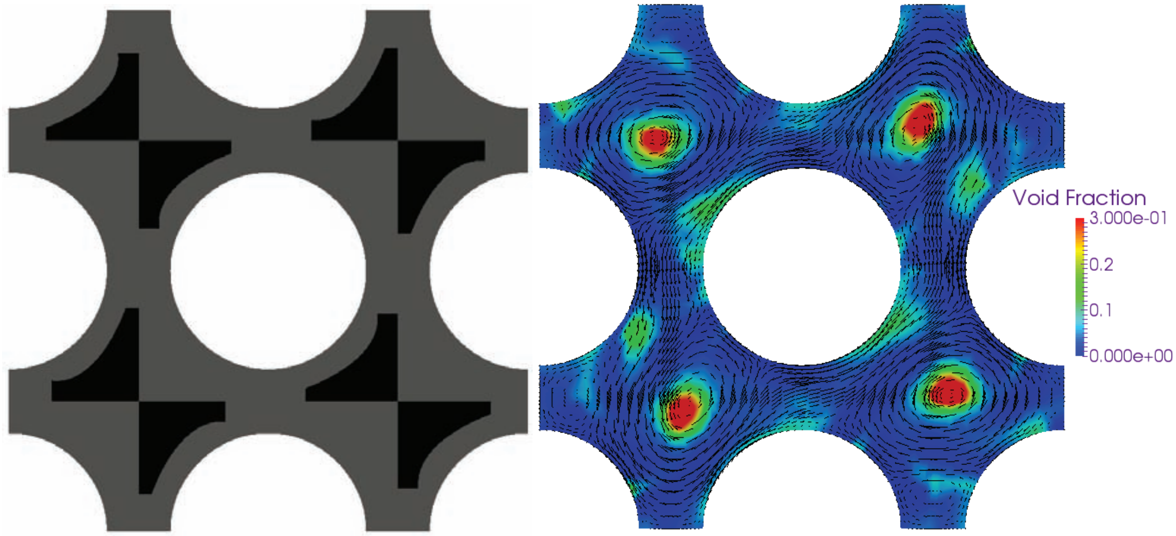


**Figure 9. Left: vane arrangement, right: four-channel case 50 mm downstream.**

The results show that there is quite a bit of communication between the subchannels. There is a swirl that can be traced throughout all four channels due to the 90 degree rotation of the vanes. This large swirl has deflected the vortices within each channel off the channel center which is contrary to what was seen in a single channel case. Similar effects were observed in the experiments. The void distribution is close to what was recorded in the outer channels, although the simulation was based on assuming symmetry planes at the outer boundaries.

### 3.2. Vapor Generated on Fuel Rods

In this work, the overall interest has been on developing a consistent formulation for boiling flows in reactor subchannels. It has been demonstrated in the previous sections of the paper that the model works well for adiabatic flows in which the vapor is already present at the inlet to the channel. However, in PWRs, vapor is generated only locally along the hottest sections of the fuel rod surface. This may considerably affect the vapor distribution upstream of the spacer.

In order to investigate this issue, a model has been implemented in NPHASE-CMFD which accounts for a prescribed uniform vapor production rate on the fuel rod surfaces, referred to as the "wall-vapor generation model". In this model, the volumetric vapor generation rate can be changed parametrically to reflect the conditions that may occur in subcooled boiling. Such an approach proves particularly useful to investigate the effects of mixing vanes on the distribution of vapor generated at the heated walls. As soon as the underlying physical phenomena are fully understood, the model can be expanded to include the effect of vapor condensation caused by liquid subcooling.

The model is implemented with a mass transfer rate along the surface of fuel rods as an input parameter. The given phase change rate accounts for the net effect of the removal of liquid and the production of vapor. The spacer grid and mixing vanes have been treated as adiabatic walls with no vapor generation. Simulations have been performed for various conditions. The basic reference case is for water/steam at atmospheric pressure, and it uses a constant vapor production rate of $4.431(10^{-3})$ kg/m$^2$-s. The inlet conditions have been formulated by simulating a uniform vapor production in a bare channel with a liquid superficial velocity of 1.468 m/s. The transverse profiles for velocities, void fraction, and turbulence quantities have been recorded at the location along the flow where the vapor superficial velocity reached 0.1673 m/s, which corresponds to the relative vapor volumetric flow rate of 10%.

The results of the simulation are shown in Figure 10, where a comparison is presented between the simulation using the given-above wall vapor generation rate and the base case. In the multiple transverse slices across the flow domain, the colors of the contours represent the local vapor void fraction and the vectors are the projections of transverse velocity of the liquid on the plane normal to the flow, similar to Figure 5a. It can be seen that near the inlet, i.e., at x=-0.01, the wall-vapor generation case has practically no vapor near the center of the channel. Downstream, the expected vortical structure is produced by the fins in both the wall-vapor case and the inlet-void case. However, it takes longer for the vapor to collect near the center of the channel in the wall-vapor generation case. Interestingly, the effect of the secondary flow seems to be moving the vapor away from the "heated" wall. There is a strong indication that, by removing the vapor from the heated wall and replacing it with liquid, the mixing vanes may significantly enhance boiling heat transfer. Naturally, this effect can only be augmented if vapor bubbles start condensing in contact with the subcooled liquid near the channel center.

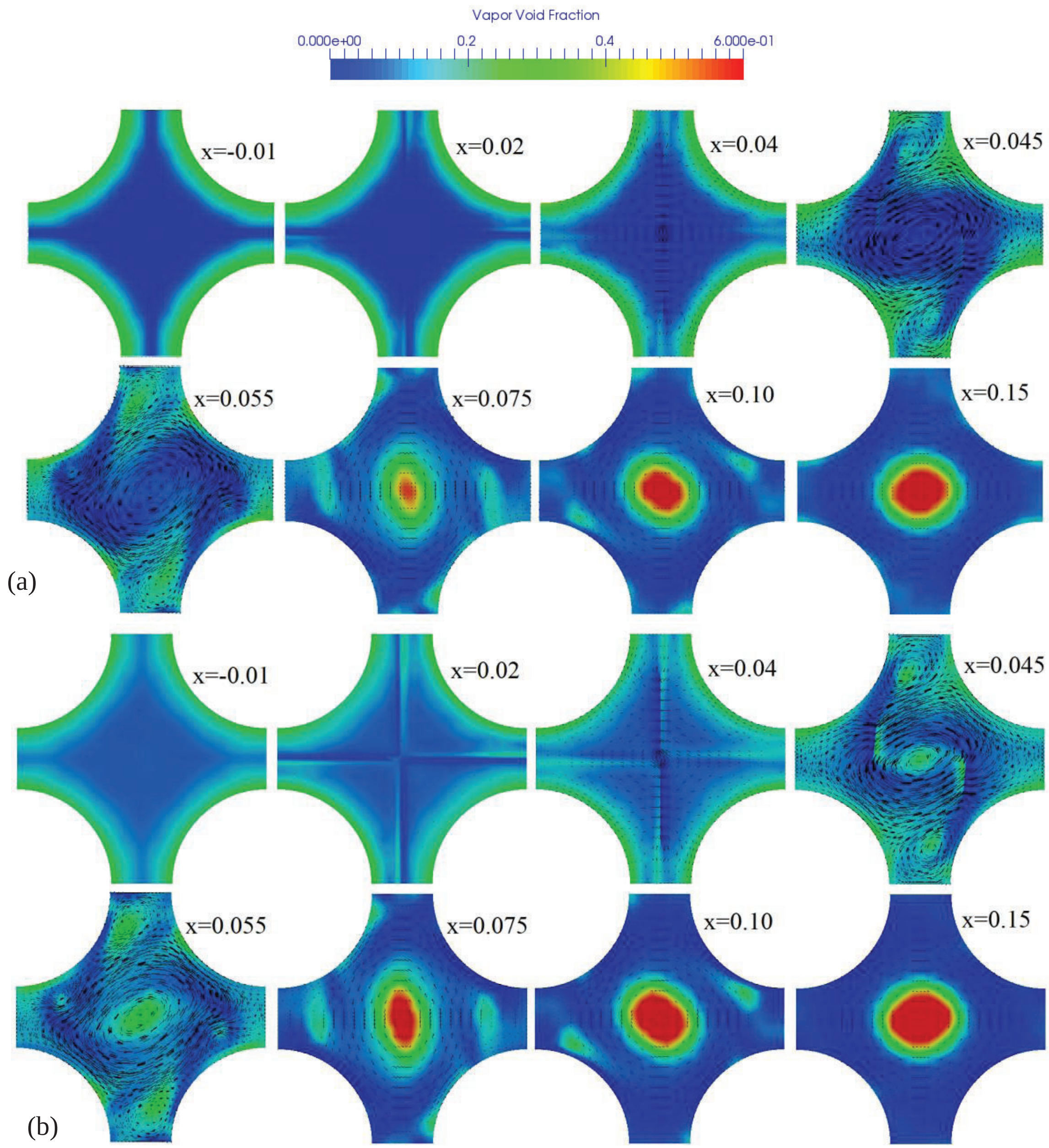


**Figure 10. Comparison of (a) vapor generated on fuel rods to (b) vapor present at inlet.**

## 4. CONCLUSIONS

The effect of mixing vanes on void distribution has been analyzed for reactor coolant channels with spacers. Valuable observations have been made how the vortex created by the mixing vanes affects the vapor phase distribution. In order for the void to re-develop, a significant distance is required for the interfacial forces to push small bubbles back toward the wall. This means that a center-peaked void would be contacting the next mixing vane as spacers could be placed about every 2 feet in a typical nuclear reactor core. The experimental validation has shown the single subchannel simulations, while still informative, are inherently limited by the prescribed symmetry boundary conditions. On the other hand, the four-parallel-channels case is capable of capturing the important effect of secondary flows around fuel rods. The low computational costs of single-channel simulations is an attractive practical factor, but a check should always be done on a larger system, as rod-bundle flows are quite complex and they are governed by phenomena occurring between the neighboring subchannels.

Accounting for wall vapor generation rate due to boiling adds an additional variable to the mixing vanes simulations as more void is continuously produced at the fuel rod surface in the presence of the mixing vanes. As it has been shown, the swirl affect may significantly decrease vapor concentration in these regions. This points to future work where the combined effects of the mixing vanes and liquid subcooling are going to be modeled. A larger experimental verification effort is also needed in order to verify the models' accuracy for flows around spacers and mixing vanes.

## ACKNOWLEDGMENTS

This research was performed under the appointment of the first author as a recipient of the Rickover Fellowship Program in Nuclear Engineering sponsored by Naval Reactors Division of the U.S. Department of Energy. The authors would also like to thank the CASL program of the U.S. Department of Energy for their support.

## REFERENCES

1. P. Tiwari, S.P. Antal and M.Z. Podowski, Three-Dimensional Fluid Mechanics of Particulate Two-Phase Flows in U-bend and Helical Conduits, Physics of Fluids, 18, 4, pp.1-18., (2006)
2. E.A. Tselishcheva, S.P. Antal and M.Z. Podowski, Mechanistic Multidimensional Analysis of Horizontal Two-phase Flows, Nuclear Engineering and Design, 240, pp.405-415. (2010)
3. D. R. Shaver, M. Z. Podowski, "Multidimensional Modeling of Forced Convection Subcooled Boiling in Pressurized Water Reactors," Proc. 2014 ANS Winter Meeting, Anaheim, CA, USA (2014)
4. M. Navarro and A.A. Santos. Evaluation of a numeric procedure for flow simulation of a 5x5 PWR rod bundle with a mixing vane spacer. Progress in Nuclear Energy, 53, pp 1190-1196. (2011)
5. M. R. Nematollahi, M. Nazifi, "Enhancement of heat transfer in a typical pressurized water reactor by different mixing vanes on spacer grids", Energy Conversion and Management 49 (2008)
6. B. Soo Shin, S. Heung Chang, "CHF experiment and CFD analysis in a 2 x 3 rod bundle with mixing vane", Nuclear Engineering and Design 239 (2009)
7. Karoutas, C. Y. Gu, et al. , "3-D Flow Analyses for Design of Nuclear Fuel Spacer", Proceedings: Seventh International Meeting on Nuclear Reactor Thermal-Hydraulics (NURETH-7), Saratoga, New York (1995):
8. H. Anglart, O. Nylund, N. Kurul, and M.Z. Podowski. CFD prediction of flow and phase distribution in fuel assemblies with spacers. Nuclear Engineering and Design, 177:215–228, (1997)

9. J. Wheeler, A. Rau, T. Worosz, & S. Kim, Experimental Investigation on the Effects of a Spacer Grid on Single- and Two-Phase Flows, International Journal of Nuclear Energy Science and Engineering, 4 (2), (2014)
10. A. Rubin, A. Schoedel, M. Avramova, H. Utsuno, S. Bajorek, and A. Velazquez-Lozada, "OECD/NRC Benchmark based on NUPEC PWR subchannel and bundle tests (PSBT), Volume I: Experimental Database and Final Problem Specifications ,"Report NES/NSC/DOC(2010)1, US NRC, OECD Nuclear Energy Agency, (2010).
11. S. Lo and J. Osman, "CFD modelling of boiling flow in PSBT 5x5 bundle", Science and Technology of Nuclear Installations, Volume 2012, Article ID 795935, Hindawi Publishing Corporation (2012)
12. K. Goodheart, N. Alleborn, A. Chatelain, and T. Keheley, "Analysis of the Interfacial Area Transport Model for Industrial 2-Phase Boiling Flow Applications" In The 15th International Meeting on Nuclear Reactor Thermal-hydraulics, NURETH-15, (2013)
13. A. Ylönen, "High-resolution flow structure measurements in a Rod bundle", PhD Thesis, NO 20961, ETH Zurich, (2013)
14. K. Goodheart, A. Ylönen, V.D. De Cacqueray, and H-M. Prasser, "CFD Validation of Void Distribution in a Rod Bundle with Spacer", 2014 22nd International Conference on Nuclear Engineering, July 7-11, 2014, Prague, Czech Republic. (2014)
15. D. R. Shaver and M. Z. Podowski, "Modeling and Analysis of Interfacial Heat Transfer Phenomena in Subcooled Boiling Along PWR Coolant Channels," Proc. NURETH-15, Pisa, Italy (2013)
16. B. M. Waite, D. R. Shaver, and M. Z. Podowski, "Prediction of Pressure Drop and Heat Transfer around Flow Obstructions," Proc. 2013 ANS Winter Meeting, Washington, DC, USA (2013)
17. B. M. Waite, D. R. Shaver, and M. Z. Podowski, "Multidimensional Mechanistic Modeling of Fluid Flow and Heat Transfer around Spacer Grids," Proc. ICAPP 2014, Charlotte, NC, USA (2014)
18. S. P. Antal, S. M. Ettorre, R. F. Kunz, and M. Z. Podowski, "Development of a Next Generation Computer Code for the Prediction of Multicomponent Multiphase Flows". Proc. Int. Meeting on Trends in Num. And Phys. Modeling for Ind. Multiphase Flow, Cargese, France (2000).
19. M.Z. Podowski, "Multiphase Flow and Heat Transfer II" Lecture Notes, RPI, Troy, NY (2014).
20. M. Ishii, T.C. Chawla, Local drag laws in dispersed two-phase flow, Argonne Report Anl-79-105, 52. (1979)
21. D. A. Drew and R. T. Lahey, "Application of General Constitutive Principles to the Derivation of Multidimensional Two-Phase Flow Equations" Int J. Multiphase Flow, Vol 7. , 242-264 (1979)
22. H Jiao and M.Z. Podowski, "An Analysis of Multidimensional Models of Gas/Liquid Flows", Proc. Amer. Nucl. Soc. Winter Meeting, vol. 107, 1393-1394, San Diego, CA, (2012).
23. S. K. Wang, S. J. Lee, O. C. Jones, and R. T. Lahey Jr. , "3-D Turbulence Structure and Phase Distribution Measurements in Bubbly Two-Phase Flows," Int. J. of Multiphase Flow, Vol 7, 243-264 (1987)
24. M. Z. Podowski, "On the Consistency of Mechanistic Multidimensional Modeling of Gas/Liquid Two-Phase Flows," Nuclear Engineering and Design, 239,933-940 (2009)
25. D. R. Shaver and M. Z. Podowski, "A Fundamental Model for Predicting Bubble Size in Diabatic Multiphase Flows, " Proc. 2013 ANS Winter Meeting, Washington, DC, USA (2013)